CARBON NANOTUBE-COMPOSITE WAFER BONDING FOR ULTRA-HIGH EFFICIENCY III-V MULTIJUNCTION SOLAR CELLS

Andreea Boca[1], Joseph C. Boisvert[1], Daniel C. Law[1], Shoghig Mesropian[1], Nasser H. Karam[1], William D. Hong[1], Robyn L. Woo[1], Dhananjay M. Bhusari[1], Evgeniya Turevskaya[2], Patrick Mack[2], and Paul Glatkowski[2]
[1]Boeing-Spectrolab, Inc., Sylmar, CA, U.S.A.; [2]Eikos, Inc., Franklin, MA, U.S.A.

ABSTRACT

Device-wafer bonding provides a platform for the implementation of ultra-high-efficiency multijunction solar cell designs, by allowing optimal subcell bandgap combinations to be attained while using only high-quality materials lattice-matched to their growth substrates. One promising new method for achieving wafer bonding is to use carbon nanotube composite thin films as the bonding agent between subcells grown on dissimilar substrates. In this paper we present the first demonstration of CNT-composite bonding of III-V materials, and evaluate its suitability for solar-cell integration in terms of optical transparency, electrical conductivity, bond uniformity and robustness, and bonded-device electrical performance. Another, relatively more mature method for device-wafer integration is that of direct semiconductor bonding technology. In order to provide a basis for comparison with CNT-bonding, we also summarize the latest achievements of the SBT solar cell development effort at Spectrolab.

INTRODUCTION

The current state-of-the-art in high-efficiency space and terrestrial III-V solar cells consists of multijunction structures in which all the component subcells are grown lattice-matched to a single substrate. This configuration limits the material choices and hence the band gap combinations available for solar cell design, and leads to sub-optimal power-conversion efficiencies. The use of metamorphic materials provides a way to dispense with the single-lattice-constant constraint, while still growing all the subcells monolithically onto a single substrate. However, metamorphic growth presents several disadvantages: it is more challenging than its lattice-matched counterpart, it cannot be used for arbitrarily large lattice mismatch with the growth substrate, and it typically introduces material defects, which may impact the performance and reliability of the overall device. One solution to this problem is to dispense with the single-substrate constraint altogether. Instead, one should start out with a design which splits the solar spectrum into the optimal bandgap combination, grow each component lattice-matched onto the most suitable substrate, and only then integrate all the subcells into a multijunction device.

In this paper, we focus on one particular such integration technology, currently under development at Spectrolab: using optically transparent, electrically conductive carbon nanotube (CNT) composite thin films as a wafer-bonding agent. We also compare this novel technique to that of semiconductor-bonding technology (SBT), and present the latest Spectrolab results on SBT high-efficiency multijunction solar cells.

CNT-based bonding offers a number of proven or potential advantages compared to other approaches to the integration of subcells grown onto different platforms. For instance, compared to SBT, CNT-integration may allow for better manufacturability, with the associated yield improvements; better thermal mismatch compliance; and relaxed epi-layer surface morphology requirements for low-defect bonding. However, while the CNT-bonding technology is now only in the early stages of development, the SBT technology is significantly more mature, with high measured efficiencies already demonstrated, e.g. 31.7% AM0 in a five-junction [1] and (see device section below) 31.4% AM0 in a four-junction bonded solar cell.

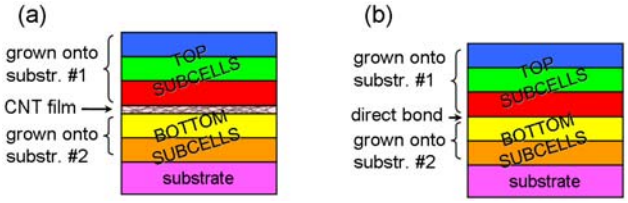

Figure 1. Multijunction cell integration: (a) CNT-composite bonding; (b) direct semiconductor bonding technology.

Figure 1a schematically shows an example consisting of a number of high-bandgap top subcells which have been grown at the lattice constant of substrate type #1, as well as of a number of lower-bandgap bottom subcells which have been grown at the different lattice constant of substrate type #2. The top and bottom subcells are bonded together by way of a thin-film CNT interface, which enables the implementation of ultra-high efficiency multijunction solar cell designs. For comparison, Fig. 1b shows the schematic of an SBT cell, wherein the top and bottom subcells are integrated into a multijunction device via direct semiconductor-to-semiconductor bonding.

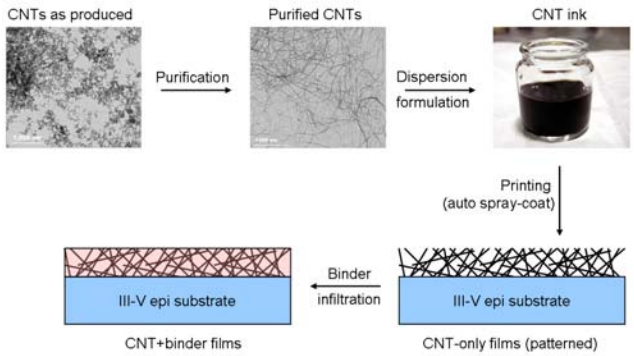

Figure 2. Eikos CNT-composite film deposition process, from the as-produced source material to binder infiltration.

The CNT materials used in this project have been provided by Eikos, Inc. in the form of Invisicon® thin films [2]. The films consist of a porous network of single-walled CNT bundles 1-2 nm in diameter and >1 μm long. These materials exhibit a broad range of tunable sheet

conductivity values 1-10^7 Ω/□, corresponding to a variety of optical transparencies, generally >90% over broad spectral regions, especially in the near-infrared. The film thickness is typically in the range 10-100 nm, with thinner films tending to have higher transparency. The CNT-film networks consist of roughly 50% nanotubes and 50% void space by volume. The voids can be infiltrated with any of a variety of so-called "binder" materials. These binders offer the film additional mechanical durability and give it an extra level of optical tunability. Examples of binders include metal oxides, metal nitrides, polymers, and inorganic-organic hybrids.

The Eikos CNT film process, schematically shown in Fig. 2, starts out with as-produced commercially available carbon nanotubes. These materials then undergo a purification process, followed by CNT-ink dispersion and formulation. The ink is spray-coated onto substrates such as III-V epitaxial semiconductors or reference glass slides, and can be patterned if necessary. The resulting CNT-only films are then infiltrated with binders in liquid solution, and cured to obtain the final CNT-binder composite films.

In order for the CNT film at the bonding interface to be suitable for the intended solar-cell integration application, it needs to satisfy three key requirements: (1) optical transparency: high-transmission for the wavelengths relevant to any solar cell active layers located underneath the film; (2) electrical conductivity: low vertical layer resistance and low-resistance ohmic contact to the semiconductor materials on either side of the nanotube film; and (3) integration capability: the ability to act as a bonding agent for solar-cell devices with superior mechanical properties and robustness. The following sections focus on CNT-film characterization results we have obtained in terms of these three requirements, and conclude with preliminary device-level test results for both CNT-based and SBT multijunction cells.

CNT-FILM OPTICAL TRANSPARENCY

The optical transmission $T_{CNT+glass}(\lambda)$ of glass slides coated on one side with CNT-only films (no binder added) was measured in a spectrophotometer as a function of wavelength, over the spectral range relevant to multijunction solar cells. The CNT films were of the same thickness, purity and material type, and were deposited using the same processes as for all the other experiments reported herein. The optical transmission of bare glass-slide substrates $T_{glass}(\lambda)$ was also measured as a baseline. An example of such a measurement is shown in Fig. 3, which also shows an estimate of the transmission of a would-be stand-alone CNT-film, calculated simply as $T_{CNT\text{-}only} = T_{CNT+glass} / T_{glass}$.

The measurement shows that the film has excellent transmission, especially in the near infrared spectral region $\lambda > 800$ nm, for which the estimated optical transparency averages in excess of 95%. We also performed optical simulations which confirmed that when incorporated into a III-V stack the CNT film including a binder would maintain its high transparency.

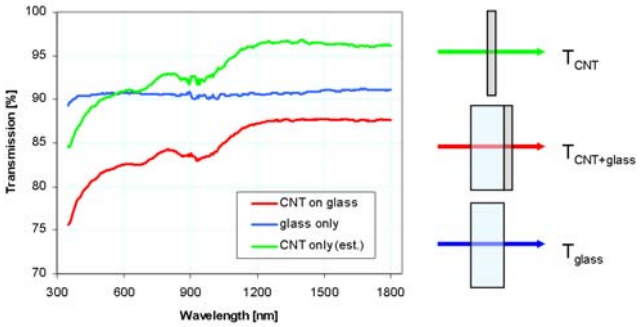

Figure 3. Measurement of CNT-film optical transparency.

The transmission characteristic can be used to estimate the performance of a multijunction solar cell in which a CNT film of this type is used to bond the narrow-bandgap subcells to the wide-bandgap ones. As an example, we consider a five-junction cell design in which the solar spectrum is divided up by the bandgap combination 2.0/1.7/1.4/1.0/0.8 eV, similar to that of Ref. [1]. We start out with a 35.0%-efficient space solar cell design as shown in the LIV simulation of Fig. 4, which assumes 20% and 25% excess current density in subcells 4 and 5 respectively, over that of current-limiting subcell 1. We then reduce the light available to the bottom two subcells by 5%, as represented by the thinner S4 and S5 LIV traces in the figure. This simulates the effect of a 95%-transmissive CNT film at the interface between subcells 3 and 4, while keeping all other simulation parameters constant. We find that the resulting calculated multijunction cell efficiency would be 34.9%, nearly the same as if the CNT film had had perfect transparency. The difference in fill factor is so slight that it can only be visualized by zooming in on the 5J LIV curve, as shown in the inset.

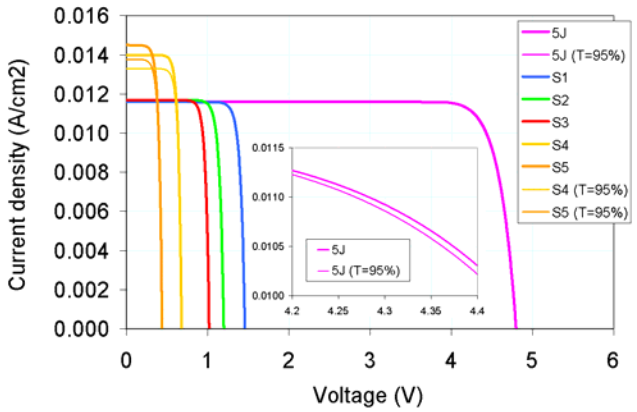

Figure 4. Simulated-LIV comparison between a 95% and a 100%-transparent CNT film in a 35%-efficient solar cell.

We therefore conclude that CNT films of this type, if used as a bonding agent, have sufficiently high transparency to support ultra-efficient solar cell designs such as the five-junction one considered here.

CNT-COMPOSITE VERTICAL CONDUCTIVITY

The in-plane or sheet conductivity of Eikos CNT films has already been well characterized in previously published work [2]. However, for the wafer-bonding application, high out-of-plane or vertical conductivity is also a key requirement. In particular, the contact resistance between the nanotube film and the epi-layers on either side, and also the vertical resistance of the film itself must be low enough to support the current-carrying needs of the multijunction device.

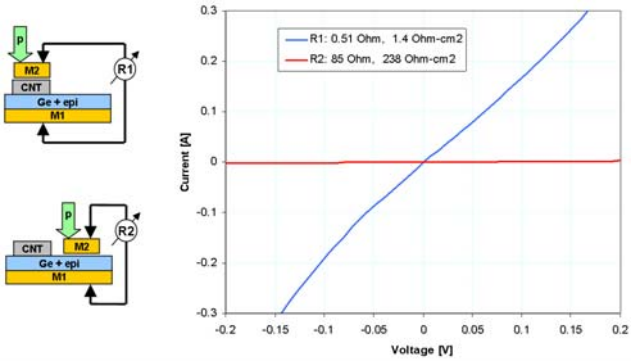

Figure 5. Test setup and IV data for CNT vertical/contact resistance measurement on an unbonded sample.

To measure the CNT vertical and semiconductor-contacting electrical properties, we deposit a nanotube film of the same type and thickness as for the samples in the previous section, except this time instead of glass the substrate is a III-V epitaxial layer grown on Ge. Metallic contacts on the top side of the CNT film (M2 in Figure 5) and on the back side of the semiconductor (M1) allow for current-voltage electrical measurements for determining the entire multi-layer stack conductivity. The total measured resistance is $R_{Tot} = R_{M2} + R_{M2\text{-}CNT} + R_{CNT} + R_{CNT\text{-}S} + R_S + R_{S\text{-}M1} + R_{M1}$, which includes the vertical (out-of-plane) resistances of all the layers, as well as the contact resistances between any two adjacent layers. Note that R_{Tot} is an upper bound on the CNT-introduced resistance that we are interested in for the bonding application, $R_{CNT} + R_{CNT\text{-}s}$, which is the sum of the CNT layer resistance and the CNT contact resistance to the semiconductor. This upper bound will be close to the value of interest $R_{CNT} + R_{CNT\text{-}S}$ if all other resistances that compose R_{Tot} are negligible in comparison.

Since CNT films (especially without a binder) are inherently porous, we avoided using deposited top contacts which may have skewed the measurement results by creating spurious electrical conductivity paths to the epi substrate through the thin nanotube film. We therefore used mechanically stacked contacts instead, and monitored the pressure applied to them during the current-voltage (IV) sweep, which ensured a resistance measurement reproducibility error of 20-30%. With this technique, we found that CNT films with or without a binder give the same vertical resistance results within the measurement error. The IV data represented by the blue curve in Figure 5 was taken on a CNT-only film area of 2.8 cm^2; an M2 contact matching the CNT film in surface area was held down by an applied pressure of 130 kPa. The upper bound to the CNT vertical and contact resistance obtained this way was R_1 = 1.4 Ω-cm^2. As a control, we also measured the resistance obtained by bypassing the CNT film and contacting the top side of the epi-substrate directly, as illustrated by the red curve in Figure 5, and obtained a resistance of R_2 = 238 Ω-cm^2. The fact that R_2 is much higher than R_1 confirms that the low resistance obtained when the CNT film is interposed between the semiconductor and the top metal contact is due indeed to the contacting properties of the nanotubes, and not to any spurious shorting paths. We therefore conclude that low-resistance ohmic contact between the III-V epi-layer and the CNT film has been achieved.

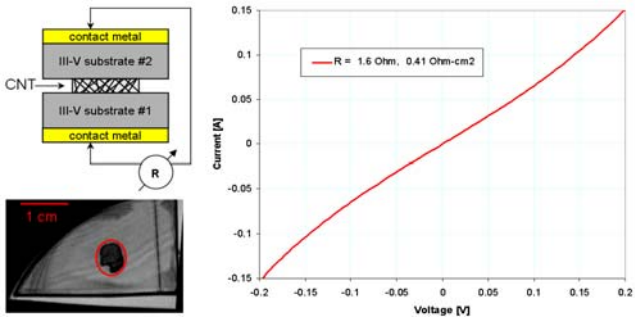

Figure 6. Test setup, SAM image, and IV curve for vertical resistance measurement on a CNT-bonded sample.

We also did a variation on this type of vertical conductivity measurement, by using CNT-bonded samples, as shown in the schematic in figure 6. In this case, we find that the measurement reproducibility error is significantly reduced as compared to the mechanically-stacked case, to less than 1%. The test structure now consists of two small-area nominally-identical III-V substrates bonded together by way of a CNT-binder composite film, with metal contacts deposited on both the front and the back sides. Therefore, the total-stack resistance is $R_{Tot} = 2\times (R_M + R_{M\text{-}S} + R_S + R_{CNT\text{-}S}) + R_{CNT}$. The IV curve in Fig. 6 was taken with no external pressure applied, on a bonded sample of total area ~4.3 cm^2. The relevant area of contact is however significantly smaller than the total sample area, due to non-uniformity of the bond in this test sample (although much better-uniformity bonds than this were later achieved on large-area wafers, as detailed in the bonding section below). The bonded area, determined through scanning acoustic imaging (SAM), is ~0.26 cm^2, as shown within the red oval in Fig. 6. Since the total-stack resistance sets an upper bound on $R_{CNT} + 2\times R_{CNT\text{-}S}$, we conclude that the specific contact resistance between the CNT film and the III-V substrate is less than 0.21 Ohm-cm^2.

Through separate measurements which we will not detail here (e.g., using CNT films deposited onto smooth metallic, rather than semiconductor substrates, or III-V layers with metallic contacts but no CNT films) we found

that all other vertical resistances included in both the bonded and the unbonded-sample R_{Tot} are negligible compared to the contact resistance R_{CNT-S}. Note that this is true, in particular, of the vertical resistance R_{CNT} of the CNT-binder composite thin film.

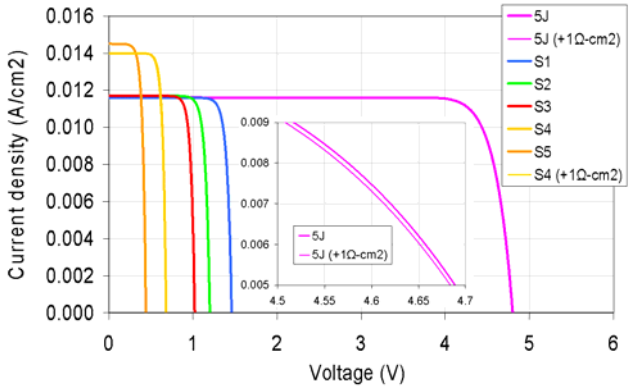

Figure 7. LIV simulation estimating the efficiency loss due to a 1 Ω-cm^2 CNT film in a 35%-efficient solar cell.

To determine the suitability of the as-measured level of vertical conductivity for the high-efficiency solar cell design in Fig. 1, we did a simple LIV simulation similar to that in Fig. 4, except this time instead of varying the CNT-layer transparency, we varied its series resistance. Starting out with the same 35.0%-efficient AM0 design, we added a 1 Ω-cm^2 series resistance to the multijunction stack, as shown in Figure 7, and found that the resulting efficiency change was less than 0.1% absolute. While better vertical conductivities would be needed for operation at high concentrations, we do conclude from this estimate that the electrical properties of current-status CNT-films are sufficient to support one-sun space or terrestrial applications.

CNT- BINDER WAFER BONDING

Figure 8a shows a typical example of the current status of CNT-composite wafer bonding at Spectrolab. Shown is the infrared (IR) transmission image of a pair of 3-inch diameter GaAs wafers. The dark, roughly circular area surrounded by fringes in the center zone of the wafer pair is a trapped void, the lighter-colored region in the mid-section is bonded, and the region around the wafer edge is unbonded (delaminated). The identification of these regions in the wafer pair as bonded or unbonded has been confirmed via scanning acoustic imaging. The CNT-bonding current baseline is reproducible and typically yields wafer pairs with 60% or more of the surface area well bonded. For comparison, figure 8b shows a typical example of a similar wafer pair bonded by way of SBT, with excellent uniformity and over 90% of the wafer pair surface area well bonded.

In order to make a preliminary assessment of the CNT-composite wafer-bond robustness when subjected to temperatures typically used as part of the multijunction cell fabrication processes, we treated a bonded wafer pair to a succession of rapid thermal anneal steps with maximum temperatures from 250 to over 430°C. The bond was IR-imaged after each step, and was seen to suffer little or no degradation, with approximately 2% bonded-area loss after the entire series.

The CNT-based wafer bond was also shown to survive through anti-reflection (AR) coating and metal deposition, as well as selected wet-etch processes with no observable degradation. The lap-shear strength of the bond was measured as well; due to equipment limitations, at this time only a lower bound was obtained, namely that the specific strength of the bond is in excess of 0.5 MPa.

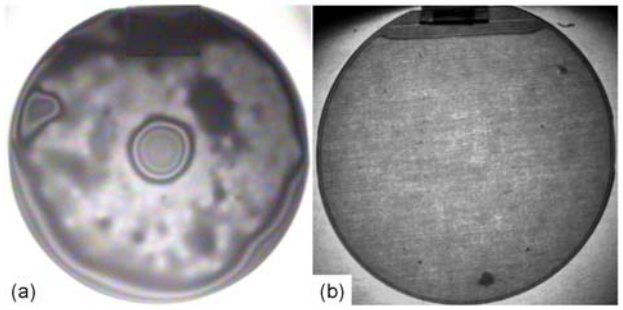

Figure 8. IR-transmission images of 3-inch diameter wafer pairs bonded by way of (a) CNT-composite films; (b) SBT.

As a preliminary assessment of the bond robustness under operating conditions, the thermal shock behavior of a pair of CNT-composite bonded wafers was also studied. The pair was alternately submerged into a cold liquid nitrogen bath at -196°C and placed onto a hot plate in air at +150°C, for 10 hot and 10 cold cycles of 1 minute each in duration. Less than 2% of the bonded areal fraction was lost over the first two cycles, with no further observable degradation suffered over the remaining eight. We have also performed thermal stress modeling on the CNT-composite bonded multijunction cell, which confirms the preliminary indications we have observed so far, of robustness under the thermal conditions expected under both processing and operating conditions.

CNT vs. SBT MULTIJUNCTION DEVICES

One incarnation of a CNT-bonded structure such as that shown in Fig. 1a is a five-junction device in which the top three subcells are grown inverted on GaAs, and the bottom two subcells are grown upright on InP substrates. Note that this would be the CNT-bonded analog of the SBT device of Ref. [1]. The successful fabrication of such a CNT-bonded five-junction device will require further development work, specifically towards verifying the compatibility of all the cell processing steps with this type of bonding. However, even before that work is complete, we proceeded with a proof-of-principle demonstration of the feasibility of CNT-bonded multijunction devices, by fabricating the structure schematically shown in Fig. 9a.

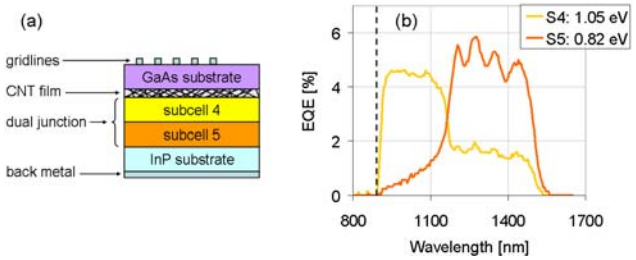

Figure 9. A first-demonstration, simplified CNT-bonded multijunction cell: (a) schematic; (b) measured SR data.

This is a dual-junction, simplified version of the target structure, in which the top three subcells are replaced by an n-type doped bare GaAs substrate; this substrate simply acts as an electrical conductor, as well as an optical filter duplicating the light absorption in the top three subcells. The bonded pair was processed with top gridline and blanket back metal contacts, which enabled characterization by spectral response (SR), as shown in Fig. 9b. The dotted vertical line represents the absorption turn-on for the GaAs substrate, coinciding with that of the third subcell in the target five-junction device. The 4-6% external quantum efficiency levels in both subcells are significantly below those needed for a high-efficiency device, which is presumably due to the lack of cell isolation in this structure, which makes it particularly vulnerable to any shunting. Nevertheless, this is the first demonstration of electrically-active, CNT-bonded multijunction solar cells, and significant performance improvements are to be expected in the near future.

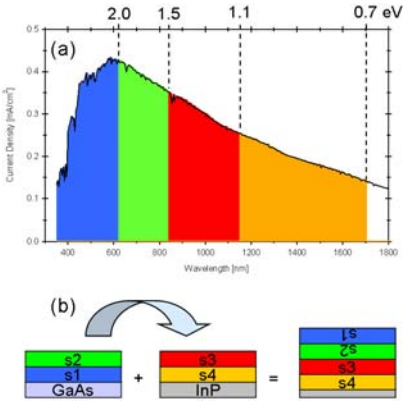

Figure 10. Four-junction SBT design: (a) AM0 spectrum splitting by bandgap combination; (b) device schematic.

As a basis for comparison, we will now briefly touch upon the current status of SBT at Spectrolab. Specifically, we will focus on a recent example, which is a four-junction (4J) SBT structure with the nominal 2.0/1.5/1.1/0.7 eV bandgap combination, which splits the AM0 solar spectrum in a near-optimal fashion, as shown in Fig. 10a. The top two subcells were grown inverted and lattice matched to GaAs, and the bottom two were grown upright and lattice matched to InP substrates. The wafers were direct-bonded, the GaAs substrate was removed (see Figure 10b), and the remaining materials were fabricated into 1 cm^2 cells by way of a fast-turnaround process which yields relatively high-obscuration top contacts. The external quantum efficiency (EQE) as measured for each of the subcells on a representative 4J-SBT cell is given by solid lines, whereas the EQE estimate assuming the same materials but a low-obscuration top-contact pattern as in typical one-sun cells is given by dashed lines in Fig. 11. The spectral response measurement apparatus used for this data was set up using a NIST-calibrated Si standard between 350-1000 nm, as well as a NIST-traceable Ge standard between 800-1800 nm.

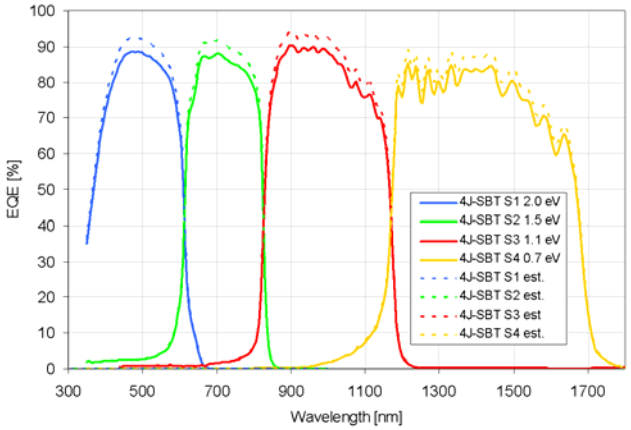

Figure 11. Four-junction SBT spectral response, as measured (solid) and as estimated (dashed).

The as-measured illuminated current-voltage (LIV) characteristic for the cell in Fig. 11 is shown by the data points in Fig 12a, where we should note that in this case the simulator was set-up using ITJ calibration standards. We find open-circuit voltage Voc = 3.433 V, short-circuit current Jsc = 14.4 mA, and fill factor FF = 0.861, leading to a 1-sun efficiency of 31.4%. Unfortunately, at this time balloon-traceable calibration isotypes even remotely matching either of the four subcells in this particular multijunction design are not available to us. Therefore, we do not have the means to setup our solar simulators for an AM0-representative measurement on these 4J-SBT cells, which means that the above as-measured LIV data should be considered best-effort. This data is, however useful for extracting a true-AM0 efficiency estimate from it, by relying on numerical simulations based on solutions to the diode equation for each subcell. The solid line in Fig. 12a is a fit to the measured LIV data; the diode parameters for each subcell (e.g., material band-gap, saturation current, effective ideality factor, shunt and series resistance), were obtained from simultaneous fits to data taken on bonded 4J and unbonded Top-2J and Bottom-2J components, under a variety of simulator calibrations. By keeping the subcell parameters fixed and only varying the color balance in order to match the integrated spectral response currents from Fig. 11, we obtain the solid line in Fig. 12b, which is our best estimate of what this exact same cell would look like under a properly-calibrated AM0 simulator. The 4J-SBT LIV parameters now become Voc = 3.394 V, Isc = 14.7 mA and FF = 0.834, yielding a true-AM0

efficiency of 30.8%. We can also estimate the performance of this cell, had it been processed with low-obscuration top contacts, as shown by the dashed line in Fig. 12b, which should be viewed as the current status of the 4J-SBT materials independent of processing details: Voc = 3.400 V, Isc = 15.3 mA, FF = 0.834, and true-AM0 efficiency 32.2%. Based on these considerations, we estimate that the present-status 4J-SBT performance surpasses that of the CNT-bonded devices described above, and likely exceeds that of the 5J-SBT cells from Ref. [1].

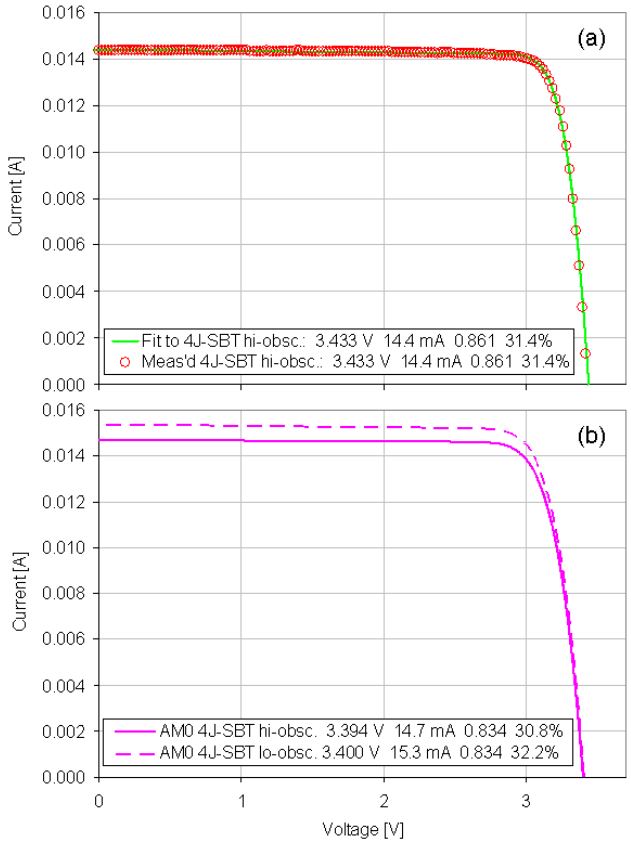

Figure 12. 4J-SBT LIV: (a) measured data and numerical fit; (b) estimated performance for true-AM0 spectrum.

CONCLUSIONS

We have summarized the current status of our CNT-composite wafer-bonding project. We have measured the optical transparency of thin CNT films and found it to be in excess of 95% over the near-infrared spectral region of interest. The vertical electrical properties of these films were also characterized, with specific contact resistances to III-V epitaxial films of less than 0.21 Ω-cm^2. The films were found to reproducibly achieve large-area wafer bonding, with improved bond uniformity expected for the near term. Proof-of-principle CNT-bonded devices have also been fabricated and tested, with further process development needed in order to bring the performance of such devices up to par with that of their SBT counterparts. For comparison, we touched upon some results from the SBT development project, which has recently demonstrated 4J cells with as-measured one-sun efficiency of 31.4% AM0.

We conclude that CNT-binder composite films represent a promising new approach for achieving wafer bonding and ultimately ultra-high efficiencies in III-V solar cell devices.

ACKNOWLEDGEMENTS

The authors would like to thank the entire R&D teams at Spectrolab and Eikos for their valuable contributions. We would also like to acknowledge the U.S. Government and the Air Force Research Laboratory for funding support.

REFERENCES

[1] D. C. Law et al., “Wafer-Bonded III-V Multijunction Solar Cells”, *34th IEEE PVSC*, 2009.

[2] P. Glatkowski et al., “Carbon Nanotube Transparent Electrodes: a Case for Photovoltaics”, *34th IEEE PVSC*, 2009.